Transaction B: Mechanical Engineering
Vol. 17, No. 4, pp. 315–326

Research Note

Optimal Trajectory Planning with the Dynamic Load Carrying Capacity of a Flexible Cable-Suspended Manipulator

M.H. Korayem[1,*], E. Davarzani[1] and M. Bamdad[1]

Abstract. *This paper presents an indirect method for computing optimal trajectory, subject to robot dynamics, flexibilities and actuator constraints. One key-issue that arises from mechanism flexibility is finding the Dynamic Load Carrying Capacity (DLCC). The motion planning problem is first formulated as an optimization problem, and then solved using Pontryagin's minimum principle. The basic problem is converted to the Two-Point Boundary Value Problem (TPBVP), which includes joint flexibility. Some examples are employed to compare three models, dynamic, flexible joint, and rigid. The results illustrate the effectiveness of this indirect method.*

Keywords: *Path planning; Payload; Flexible cable-suspended manipulator; Optimal control; Two point boundary value problem.*

INTRODUCTION

Several advantages distinguish cable-based systems from common manipulators. First, the mechanical architecture is rather simple and cost-effective even in the case of multiple DOF spatial systems. As a further consequence, these robots often present very high payload-to-weight ratios. RoboCrane, as one of the early works on cable-actuated manipulators, was developed based on the Stewart platform parallel link manipulator, providing a precise, six degrees of freedom control of loads.

The Dynamic Load Carrying Capacity (DLCC) of a conventional serial manipulator is usually defined as the maximum load that a manipulator can lift and carry in a fully extended configuration. If the end-effector trajectory is predefined, DLCC would be the maximum value of load that the manipulator is able to carry [1,2].

1. *Robotic Research Laboratory, College of Mechanical Engineering, Iran University of Science and Technology, P.O. Box 18846, Tehran, Iran.*
*. *Corresponding author. E-mail: hkorayem@iust.ac.ir*

Received 12 September 2009; received in revised form 2 March 2010; accepted 3 May 2010

The other definition of DLCC will be obtained by finding the maximum payload that a manipulator can carry between the given initial and final position of the end-effector. In this case, finding the maximum payload and corresponding optimal path is formulated as a trajectory optimization problem [3].

In practice, the methods of solving deterministic optimal control problems are divided into two categories: direct and indirect methods. Direct methods are based on a discretization of dynamic variables (states, controls), leading to a parameter optimization problem, and it is solved by using one of the nonlinear programming codes. On the other hand, indirect methods are based on the minimum principle of Pontryagin. In this method, necessary conditions for optimality are found and the obtained equations establish a Two Point Boundary Value Problem (TPBVP) that is solved by numerical techniques [4].

There have been a number of researchers who have developed trajectory planning and dynamic modeling for cable-actuated robots. Hiller et al. studied the workspace, forward kinematics and trajectory planning of one type of planer cable robot. In his paper, the optimal path is found by using a Powell algorithm and the method of simulated annealing [5]. One typical spatial cable robot was investigated and one direct method was used for stiffness optimization and optimal trajectory planning [6]. Recently, Korayem et al. have introduced a procedure for finding the optimal path of maximum load for a cable suspended robot and a cable planar robot [7,8]. They used an indirect method and, as mentioned before, the optimization problem is converted to a two-point boundary value problem as by solving that, we can have a precise solution of the problem. This method could be used for any kind of system wherein the state space form of equations is achievable. This method is used as a competent tool for analyzing nonlinear systems and the path planning of different types of system.

On the other hand, considering flexibility in modeling, the flexibility of joints exists in all robots, so achieving better precision in the modeling and control of a robot must be considered. This kind of flexibility could be the consequence of different determinatives, such as looseness of gears and forced transmission systems (like belts and shafts), as they are determinatives of error generation between theoretical and practical results. Flexibility of joints could generate a low resonance frequency in the structure and unwanted vibrations in the robot. Towards this end, Korayem and Nikoobin devoted themselves to finding the optimal path of a two link manipulator by considering the flexibility of joints. This paper also used the optimal control method and the minimum principle of Pontryagin [9].

Flexible manipulators vibrate not only during tracking, but also after reaching the goal point. Korayem et al. investigated this residual vibration, which continues with a specific amplitude and frequency after reaching the goal point and the effect of this on the carried payload [10]. The stiffness and stability of cable-suspended manipulators with application to load optimal determination are studied. Korayem and Bamdad addressed computation of the maximum load carrying capacity of large cable-suspended parallel manipulators [11].

Among numerous papers in the field of parallel manipulator path planning, flexibility in the joint has rarely been considered. Moreover, in no previous work in the area of cable-suspended parallel robots, has joint flexibility been considered in the dynamic equation.

In this paper, the problem of the optimal path and maximum dynamic load carrying capacity of a sample spatial cable robot is studied. The open loop optimal control approach is applied, and using the indirect method and Pontryagins' minimum principle, the original problem is converted to a two-point boundary value problem. A number of simulations for a cable-suspended manipulator with flexible joints are carried out to investigate the efficiency of the presented method.

The paper is organized as follows: First, the dynamic modeling of a system, considering the flexibility of joints, for one type of six cable spatial robot, is introduced. Then, the optimal control problem and necessary conditions for optimality are dealt with. Then, based on the solution of TPBVP, an algorithm is developed for finding the optimal path for a specific payload and another is then given for determining maximum payload and corresponding optimal path. Finally, simulation results are presented and discussed including verification.

PROBLEM FORMULATION

In cable-suspended manipulators, the weight of the end-effector provides tension in the cables. The type of cable robot is as an Incompletely Restrained Parallel Manipulator, IRPM, because the kinematics of the robot are not sufficient to completely restrain the end-effector and, thus keep all cables in tension. Since the end-effector has six degrees of freedom, the minimum number of cables or actuators is six.

First, the dynamic model of a typical cable-suspended robot will be presented and, then, the effects of flexible joints are exerted in an ideal model. Finally, the full dynamic model is derived. The paper will be continued with the formulation of necessary conditions for optimality.

Dynamic Modeling of Spatial Cable Robot

A spatial cable robot has a triangular shaped end-effector, as shown in Figure 1, which is suspended through 6 cables and has 6 degrees of freedom. If we show the direction and position of the end-effector relative to the reference coordinate by six variables of $X = [x, y, z, \psi, \theta, \phi]^T$, cable length by $l = [q_1, q_2, q_3, q_4, q_5, q_6]^T$ and cable tension by $T = [T_1, T_2, T_3, T_4, T_5, T_6]^T$, the dynamic model of the sys-

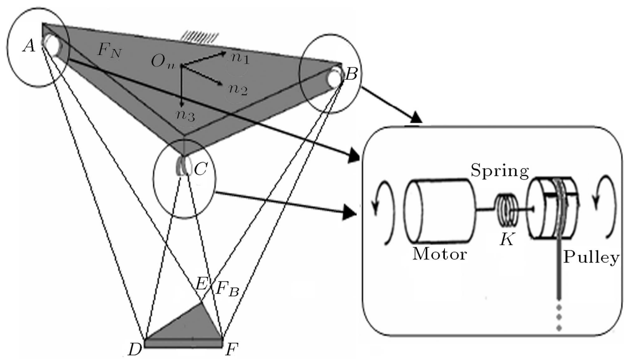

Figure 1. Six cable spatial robot with flexible joints [6].

tem will be as follows [1,6]:

$$D(X)\ddot{X} + C(X,\dot{X}) + G(X) = -J^T(X)T,$$

$$J = \begin{bmatrix} \frac{\partial q_1}{\partial x} & \frac{\partial q_1}{\partial y} & \frac{\partial q_1}{\partial z} & \frac{\partial q_1}{\partial \psi} & \frac{\partial q_1}{\partial \theta} & \frac{\partial q_1}{\partial \phi} \\ \frac{\partial q_2}{\partial x} & \frac{\partial q_2}{\partial y} & \frac{\partial q_2}{\partial z} & \frac{\partial q_2}{\partial \psi} & \frac{\partial q_2}{\partial \theta} & \frac{\partial q_2}{\partial \phi} \\ \frac{\partial q_3}{\partial x} & \frac{\partial q_3}{\partial y} & \frac{\partial q_3}{\partial z} & \frac{\partial q_3}{\partial \psi} & \frac{\partial q_3}{\partial \theta} & \frac{\partial q_3}{\partial \phi} \\ \frac{\partial q_4}{\partial x} & \frac{\partial q_4}{\partial y} & \frac{\partial q_4}{\partial z} & \frac{\partial q_4}{\partial \psi} & \frac{\partial q_4}{\partial \theta} & \frac{\partial q_4}{\partial \phi} \\ \frac{\partial q_5}{\partial x} & \frac{\partial q_5}{\partial y} & \frac{\partial q_5}{\partial z} & \frac{\partial q_5}{\partial \psi} & \frac{\partial q_5}{\partial \theta} & \frac{\partial q_5}{\partial \phi} \\ \frac{\partial q_6}{\partial x} & \frac{\partial q_6}{\partial y} & \frac{\partial q_6}{\partial z} & \frac{\partial q_6}{\partial \psi} & \frac{\partial q_6}{\partial \theta} & \frac{\partial q_6}{\partial \phi} \end{bmatrix}, \tag{1}$$

in which $J(X)$ is the conventional matrix of the robot's Jacobian, $D(X)$ is the inertia matrix of the robot, $C(X,\dot{X})$ is the vector of Coriolis and centrifugal forces and $G(X)$ is the vector of gravity forces. The cables must be capable of exerting a positive force and torque on the end effector.

Dynamic Modeling of Cable Robot with Flexible Joints

A torsional spring is considered between the motor and pulley .for the dynamics of the flexible joint. In this case, the rotation of motors and pulleys can be different, and the following relations will be from the vibration modeling of the system:

$$j\ddot{\beta} + K(\beta - \beta') = -rT, \tag{2}$$

in which K (N.m /rad) is the torsional spring coefficient, β (rad) is the motor rotation angle and β' (rad) is the pulley rotation angle. Also, we have:

$$j'\ddot{\beta}' - K(\beta - \beta') = \tau, \tag{3}$$

in which j' (kg.m^2) is motor inertia and $\ddot{\beta}'$ (rad/s^2) is angular acceleration of motors. The following equation is for the velocity and acceleration of pulleys:

$$\dot{\beta} = \frac{\partial \beta}{\partial X}\dot{X}, \qquad \frac{\partial \beta}{\partial X} = -\frac{1}{r}J;$$

$$\ddot{\beta} = \frac{d}{dt}\left(\frac{\partial \beta}{\partial X}\right)\dot{X} + \frac{\partial \beta}{\partial X}\ddot{X}. \tag{4}$$

We need to rewrite the dynamic equations into a state space equation form for solving the optimization problem. With regard to flexibility in the joints, we have 12 degrees of freedom. Therefore, there are 24 state variables defined as:

$$X_1 = \begin{bmatrix} x_1 \\ x_2 \\ x_3 \\ x_4 \\ x_5 \\ x_6 \end{bmatrix} = \begin{bmatrix} x \\ y \\ z \\ \psi \\ \theta \\ \phi \end{bmatrix}, \qquad X_2 = \begin{bmatrix} x_7 \\ x_8 \\ x_9 \\ x_{10} \\ x_{11} \\ x_{12} \end{bmatrix} = \begin{bmatrix} \dot{x} \\ \dot{y} \\ \dot{z} \\ \dot{\psi} \\ \dot{\theta} \\ \dot{\phi} \end{bmatrix},$$

$$X_3 = \begin{bmatrix} x_{13} \\ x_{14} \\ x_{15} \\ x_{16} \\ x_{17} \\ x_{18} \end{bmatrix} = \begin{bmatrix} \beta'_1 \\ \beta'_2 \\ \beta'_3 \\ \beta'_4 \\ \beta'_5 \\ \beta'_6 \end{bmatrix}, \qquad X_4 = \begin{bmatrix} x_{19} \\ x_{20} \\ x_{21} \\ x_{22} \\ x_{23} \\ x_{24} \end{bmatrix} = \begin{bmatrix} \dot{\beta}'_1 \\ \dot{\beta}'_2 \\ \dot{\beta}'_3 \\ \dot{\beta}'_4 \\ \dot{\beta}'_5 \\ \dot{\beta}'_6 \end{bmatrix}. \tag{5}$$

Now concerning these variables from Equation 1, we have:

$$\dot{X}_2 = D^{-1}(-J^T T - C - G). \tag{6}$$

By the placement of Equations 2 and 4 in the above equation and the elimination of T, we have:

$$\dot{X}_2 = \left[I_{6*6} + \frac{D^{-1}J^T jJ}{r^2}\right]^{-1}\left[D^{-1}\left\{\frac{J^T K(\beta - \beta')}{r} - C - G\right\}\right] \Rightarrow \dot{X}_2 = F_1(X_1, X_2, X_3). \tag{7}$$

It is important to note that in the placement of the second derivative of the pulley rotation angle, the non-linear term is relinquished because, firstly, in previous studies conducted, the linear term is effective and, secondly, by regarding the nonlinear term, the size of the MATLAB file becomes 30 MB, which no software can solve.

On the other hand from Equation 3 we have:

$$\dot{X}_4 = \ddot{\beta} = \frac{[\tau + K(\beta - \beta')]}{j'} \Rightarrow \dot{X}_4 = F_2(X_1, X_3, U). \tag{8}$$

Finally, state equations of the system will be as follows:

$$\begin{bmatrix} \dot{X}_1 \\ \dot{X}_2 \\ \dot{X}_3 \\ \dot{X}_4 \end{bmatrix} = \begin{bmatrix} X_1 \\ F_1(X_1, X_2, X_3) \\ X_4 \\ F_2(X_1, X_3, U) \end{bmatrix}. \tag{9}$$

Problems of Optimal Control and Necessary Condition of Optimality

In this optimal control problem, we want to determine the state function, $X(t)$, and the control function, $U(t)$. The general method is, first, for a specified load; the optimal path of the robot for moving between the primary and final point is found. Then, the maximum load is found through an iterative algorithm.

Deriving Equations for Flexible Joints Case

According to [4,7], the overall form of the objective function is as follows:

$$J_0(U) = \frac{1}{2}\|e_{p_1}(t_f)\|^2_{W_{p_1}} + \frac{1}{2}\|e_{p_2}(t_f)\|^2_{W_{p_2}} + \frac{1}{2}\|e_{v_1}(t_f)\|^2_{W_{v_1}} + \frac{1}{2}\|e_{v_2}(t_f)\|^2_{W_{v_2}} + \int_{t_0}^{t_f} L(X,U)dt, \tag{10}$$

where:

$$e_{p_1}(t_f) = X_1(t_f) - X_{1f},$$

$$e_{p_2}(t_f) = X_3(t_f) - X_{3f},$$

$$e_{v_1}(t_f) = X_2(t_f) - X_{2f},$$

$$e_{v_2}(t_f) = X_4(t_f) - X_{4f},$$

$$L(X,U) = \frac{1}{2} * (\|X_1\|^2_{W_1} + \|X_2\|^2_{W_2} + \|X_3\|^2_{W_3} + \|X_4\|^2_{W_4} + \|U\|^2_R), \tag{11}$$

where t_0 and t_f are known as the initial and final times, and the integrand, L, is a smooth differentiable function in the argument. $\|X\|^2_K = X^T K X$ is the generalized squared norm, W_p and W_v are symmetric positive semi-definite $(n \times n)$ weighting matrices, $W_1, \cdots, W_4$ and R are symmetric positive definite $(n \times n)$ matrices. X_{1f}, X_{2f}, X_{3f} and X_{4f} are the desired values of the position and velocity of the cable at the final time. The performance criteria defined by Equation 10 are minimized on the total range of motion. On the other hand, the boundary conditions at the beginning and end of the path are:

$$X_1(0) = X_{10}, \qquad X_2(0) = X_{20},$$

$$X_3(0) = X_{30}, \qquad X_4(0) = X_{40},$$

$$X_1(t_f) = X_{1f}, \qquad X_2(t_f) = X_{2f},$$

$$X_3(t_f) = X_{3f}, \qquad X_4(t_f) = X_{4f}, \tag{12}$$

which represent the position and velocity of the end-effector at the initial and final time. Each of the pulleys works on an under specific curve and in a particular range;

$$\overline{U} = \{U_i^- \leq U_i \leq U_i^+\}, \tag{13}$$

in which the upper and lower limits of the torques according to the current-torque characteristics of DC motors are defined as [1]:

$$U^+ = K_1 - K_2 X_2, \qquad U^- = K_1 - K_2 X_2, \tag{14}$$

where:

$$K_1 = \begin{bmatrix}\tau_{s1} & \tau_{s2} & \cdots & \tau_{sn}\end{bmatrix}^T,$$

$$K_2 = \mathrm{dig}\begin{bmatrix}\frac{\tau_{s1}}{\omega_{11}} & \cdots & \frac{\tau_{sn}}{\omega_{mn}}\end{bmatrix}.$$

τ_s is the still torque and ω_{mi} is the maximum no load speed of the motor. It is noticeable that since the cables are only capable of being in tension, the upper limit of the torque for our robot will be zero.

As mentioned, for solving the optimality problem, we use the indirect method, thus first the Hamiltonian function is defined as follows:

$$H = L + \Psi_1^T X_2 + \Psi_2^T F_1 + \Psi_3^T X_4 + \Psi_4^T F_2, \tag{15}$$

where:

$$W_1 = \begin{bmatrix} w_1 & \cdots & 0 \\ \vdots & \ddots & \vdots \\ 0 & \cdots & w_6 \end{bmatrix}, \qquad W_2 = \begin{bmatrix} w_7 & \cdots & 0 \\ \vdots & \ddots & \vdots \\ 0 & \cdots & w_{12} \end{bmatrix},$$

$$W_3 = \begin{bmatrix} w_{13} & \cdots & 0 \\ \vdots & \ddots & \vdots \\ 0 & \cdots & w_{18} \end{bmatrix}, \qquad W_4 = \begin{bmatrix} w_{19} & \cdots & 0 \\ \vdots & \ddots & \vdots \\ 0 & \cdots & w_{24} \end{bmatrix},$$

$$R = \begin{bmatrix} R_1 & \cdots & 0 \\ \vdots & \ddots & \vdots \\ 0 & \cdots & R_6 \end{bmatrix}, \qquad \psi_1 = \begin{Bmatrix} x_{25} \\ x_{26} \\ x_{27} \\ x_{28} \\ x_{29} \\ x_{30} \end{Bmatrix},$$

$$\psi_2 = \begin{Bmatrix} x_{31} \\ x_{32} \\ x_{33} \\ x_{34} \\ x_{35} \\ x_{36} \end{Bmatrix}, \qquad \psi_3 = \begin{Bmatrix} x_{37} \\ x_{38} \\ x_{39} \\ x_{40} \\ x_{41} \\ x_{42} \end{Bmatrix}, \qquad \psi_4 = \begin{Bmatrix} x_{43} \\ x_{44} \\ x_{45} \\ x_{46} \\ x_{47} \\ x_{48} \end{Bmatrix}, \tag{16}$$

Finally, by using the Pontryagin minimum principle, we have the following relations:

1. $\dot{X} = \frac{\partial H}{\partial \Psi} \rightarrow \begin{cases} \dot{X}_1 = X_2 \\ \dot{X}_2 = F_1(X_1, X_2, X_3) \\ \dot{X}_3 = X_4 \\ \dot{X}_4 = F_2(X_1, X_3, U) \end{cases}$

2. $\dot{\psi} = -\frac{\partial H}{\partial x} \rightarrow$

$$\begin{cases} \dot{\psi}_1 = -\left([w_1 x_1; w_2 x_2; w_3 x_3; w_4 x_4 \right. \\ \qquad w_5 x_5; w_6 x_6] + \left(\dfrac{\partial F_1}{\partial X_1}\right)^T \{\psi_2\} + \\ \qquad \left. \left(\dfrac{\partial F_1}{\partial X_1}\right)^T \{\psi_2\}\right) \\ \dot{\psi}_2 = -\left([w_7 x_7; w_8 x_8; w_9 x_9; w_{10} x_{10} \right. \\ \qquad w_{11} x_{11}; w_{12} x_{12}] + \{\psi_1\} + \\ \qquad \left. \left(\dfrac{\partial F_1}{\partial X_2}\right)^T \{\psi_2\}\right) \\ \dot{\psi}_3 = -\left([w_{13} x_{13}; w_{14} x_{14}; w_{15} x_{15}; w_{16} x_{16} \right. \\ \qquad w_{17} x_{17}; w_{18} x_{18}] + \left(\dfrac{\partial F_1}{\partial X_3}\right)^T \{\psi_2\} + \\ \qquad \left. \left(\dfrac{\partial F_2}{\partial X_3}\right)^T \{\psi_4\}\right) \\ \dot{\psi}_4 = -\left([w_{19} x_{19}; w_{20} x_{20}; w_{21} x_{21}; w_{22} x_{22} \right. \\ \qquad \left. w_{23} x_{23}; w_{24} x_{24}] + \{\psi_3\}\right) \end{cases}$$

3. $\frac{\partial H}{\partial u} = 0 \rightarrow \tau_{6*1} = -R^{-1} \left(\frac{\partial F_2}{\partial U}\right)^T \Psi_4 \rightarrow$

$$u_i = \begin{cases} U_i^+ & \tau_i > U_i^+ \\ \tau_i & U_i^- < \tau_i < U_i^+ \\ U_i^- & \tau_i < U_i^- \end{cases} \tag{17}$$

We have totally 48 differential equations, which with the last control law form all the required equations. In solving process, first of all control Equation 3 would be substituted in two other equations for a known load (Equations 17). Consequently, the resultant equations establish a set of $4n$ ordinary differential equations, while Equation 12 describes a $4n$ boundary value condition $2n$ of which are defined as $t = t_0$ and the other $2n$ as $t = t_f$. The algorithm iterates on the initial values of the costate until the final error converges to the desired accuracy, ε. To put it another way, the following relation must be satisfied by TPBVP solving:

$$\frac{1}{2}\|X_1(t_f) - X_{1f}\|^2_{W_{p1}} + \frac{1}{2}\|X_3(t_f) - X_{3f}\|^2_{W_{p2}} + \frac{1}{2}\|X_2(t_f) - X_{2f}\|^2_{W_{\nu 1}} + \frac{1}{2}\|X_4(t_f) - X_{4f}\|^2_{W_{\nu 2}} \leq \varepsilon. \tag{18}$$

ALGORITHM OF FINDING OPTIMAL PATH AND MAXIMUM PAYLOAD

Finding Optimal Path for Specific Payload

1. Select ε and penalty matrices.
2. Select two points that indicate the initial and final positions of the manipulator in the workspace of the robot, as they use in the boundary condition.
3. We go to the next step, if the workspace in two selected points does not include singularity, otherwise, if Jacobian values at the initial or final configuration are equal to zero, the algorithm jumps back to the second step and two new points should be selected (Condition I).
4. Select a primary path as the initial guess for solving the problem.
5. Solve the two point boundary value problem using the given boundary conditions and the BVP4C command in MATLAB software.
6. Calculate the amount of torque (and if necessary the other problems, such as tension of cable, length of cable etc.).
7. If the desired objectives and purposes and the required accuracy are satisfied, the obtained path is optimal and the running should be stopped, otherwise the algorithm jumps back to step 4 (Condition II).

Calculation of Maximum Payload

The algorithm of the maximum payload has also been shown in Figure 2. The first to third step of this algorithm is similar to the previous algorithm. In this algorithm, by selecting penalty matrices, maximum load is calculated per specific objective function. m_p^0 is the value of the primary load and $\Delta\mu$ determines the increasing value of the load at each stage. The solving method is based on increasing the minimum amount of load until the maximum is obtained.

SIMULATION

In this section, simulation is done for different flexibilities and under rigid conditions. It is noticeable that the rigid optimal path is used as the initial guess in each flexible case.

Simulation is done for a specific load of 13 (kg), and moving between the point (-0.1, -0.1, 1.5) and point (0.1, 0.1, 1.8) for two different flexible and rigid cases to guarantee the results. Applied boundary conditions in the simulation are according to Table 1, and other specifications are listed in Table 2. In Figure 3, comparisons between motor torques for the first and sixth ones are shown. It is clear, by considering joint flexibility, that the torques will have vibrations around the rigid torque and that, by increasing the stiffness of the modeled spring, these vibrations decrease.

Then values of the maximum load and also the required optimal path are obtained for two different flexible and rigid cases.

In this simulation, also the boundary conditions are the same as in the last simulation and Table 2. According to conducted simulations, the maximum

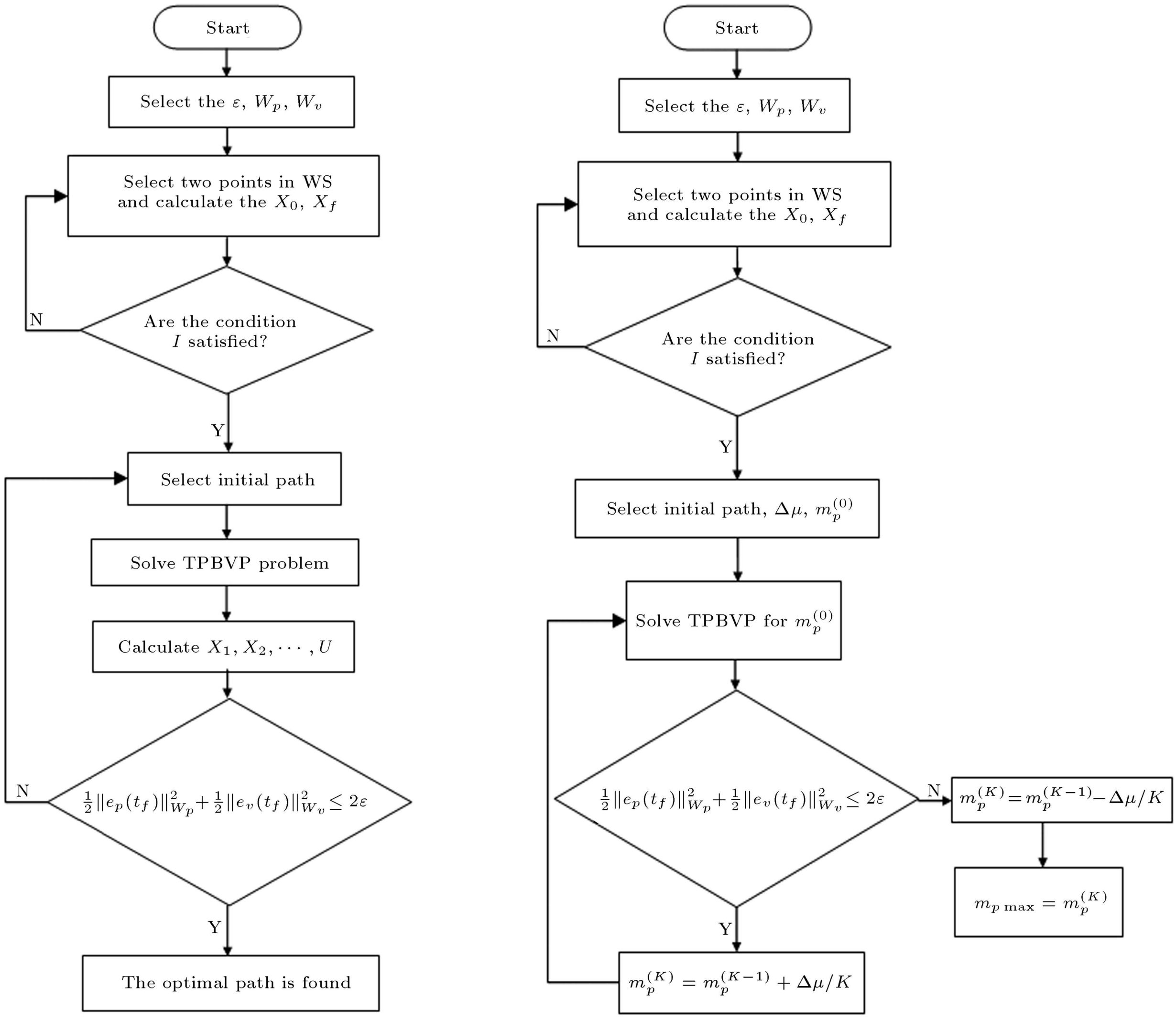

(a) (b)

Figure 2. (a) Finding optimal path for specific payload. (b) Calculation of maximum payload.

Table 1. Boundary conditions of flexible joints case.

$X_1(0) = [-0.1, -0.1, +1.5, 0, 0, 0]^T$	$X_1(t_f = 1) = [+0.1, +0.1, +1.8, 0, 0, 0]^T$
$X_2(0) = [0, 0, 0, 0, 0, 0]^T$	$X_2(t_f = 1) = [0, 0, 0, 0, 0, 0]^T$
$X_3(0) = [0, 0, 0, 0, 0, 0]^T$	For $K = 5 : X_3(t_f = 1) = [-4.693, -6.49, -5.317, -4.831, -6.482, -5.119]^T$ For $K = 20 : X_3(t_f = 1) = [-4.929, -6.849, -5.496, -4.972, -6.846, -5.417]^T$
$X_4(0) = [0, 0, 0, 0, 0, 0]^T$	$X_4(t_f = 1) = [0, 0, 0, 0, 0, 0]^T$

payload for a rigid case is obtained as 22.9 (kg), and by adding joint flexibility this value is reduced; for spring stiffness of 20 (N.m/rad), it is decreased to 19 (kg) and for spring stiffness of 5 (N.m/rad), it is decreased to 17.7 (kg). Figure 4 shows the optimal path of each case that is listed above. It should be mentioned that in each of the simulation cases, before the first motor saturation, the optimal paths of different loads are the same and, then, if the load increases, the plan attempts to change the path to still keeping the torques within the allowed range. Also, increasing the load is possible until the needed accuracy in the problem is provided. In Figure 5, for example, in spring stiffness 5 (N.m/rad), the motor torques achieve maximum payload. It is noticeable that in the case of spring stiffness equal to 5 (N.m/rad), we

Table 2. Simulation parameters in flexible joints case.

Parameter	Value	Unit
Moment of inertia (I_{xx})	$I_{zz}=\frac{\rho b^4 t}{2\sqrt{3}}+\frac{\rho b^2 t^3}{4\sqrt{3}}$	kg.m^2
Moment of inertia (I_{yy})	$I_{zz}=\frac{\rho b^4 t}{2\sqrt{3}}+\frac{\rho b^2 t^3}{4\sqrt{3}}$	kg.m^2
Moment of inertia (I_{zz})	$I_{zz}=\frac{\rho b^4 t}{\sqrt{3}}$	kg.m^2
a	0.3	m
b	0.3	m
Motor's max. no load speed	330	Rad/s
Motor stall torque	2.84	N.m
Pulley radius	0.05	m
Pulley rotational inertia	8×10^{-4}	kg.m^2
Rotational inertia for motor collection	8×10^{-4}	kg.m^2

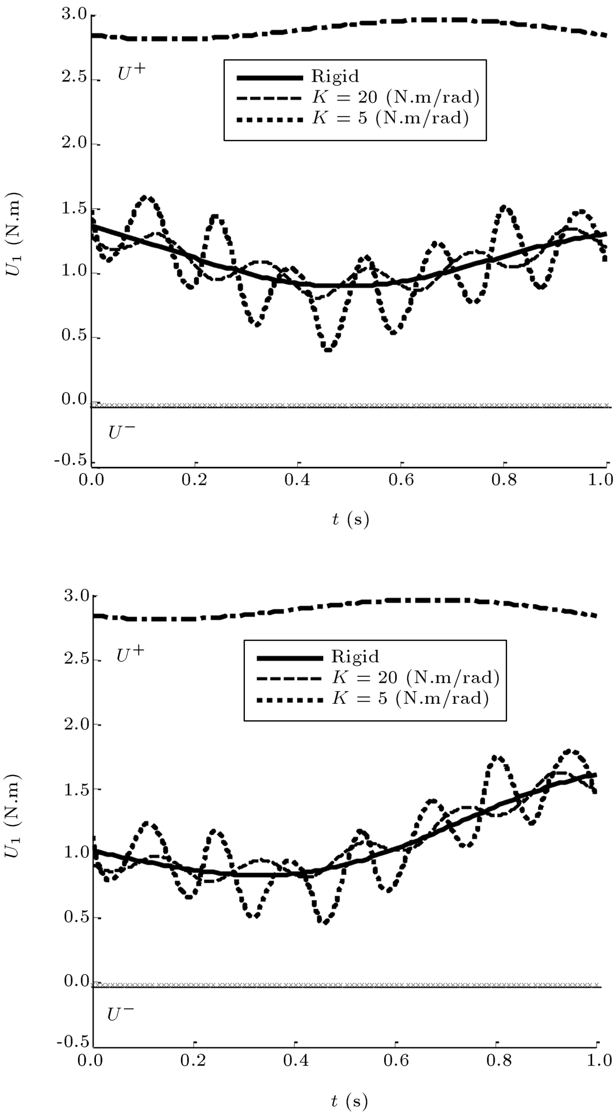

Figure 3. Comparison of motor torques in rigid and flexible joint cases for specific payload.

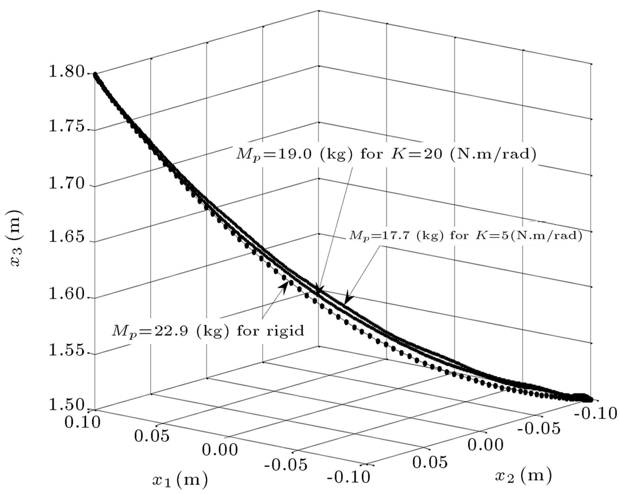

Figure 4. Optimal path for maximum payload in different cases of joint flexibility in XYZ space.

have seen, on the maximum payload, that only the fifth motor has reached the saturation limit; in the second case, the fifth motor has reached the saturation limit and the second motor is also near the end of saturation. But, in rigid cases, the 5th, 2nd and 4th motors were saturated and the 6th motor also reposed near to saturation. In this simulation, the torques tried to reach their upper bound. In Figure 6, motor torques in maximum payload for rigid cases are shown.

To evaluate the accuracy of the obtained curves, one of the methods is finding the values of the tensions that are used here. Concerning Figures 7 and 8, the tension of whole cables, when carrying the maximum load in the obtained optimal path, is positive.

As can be seen, obtained optimal paths in both flexible cases are very close to rigid optimal paths. Inci-

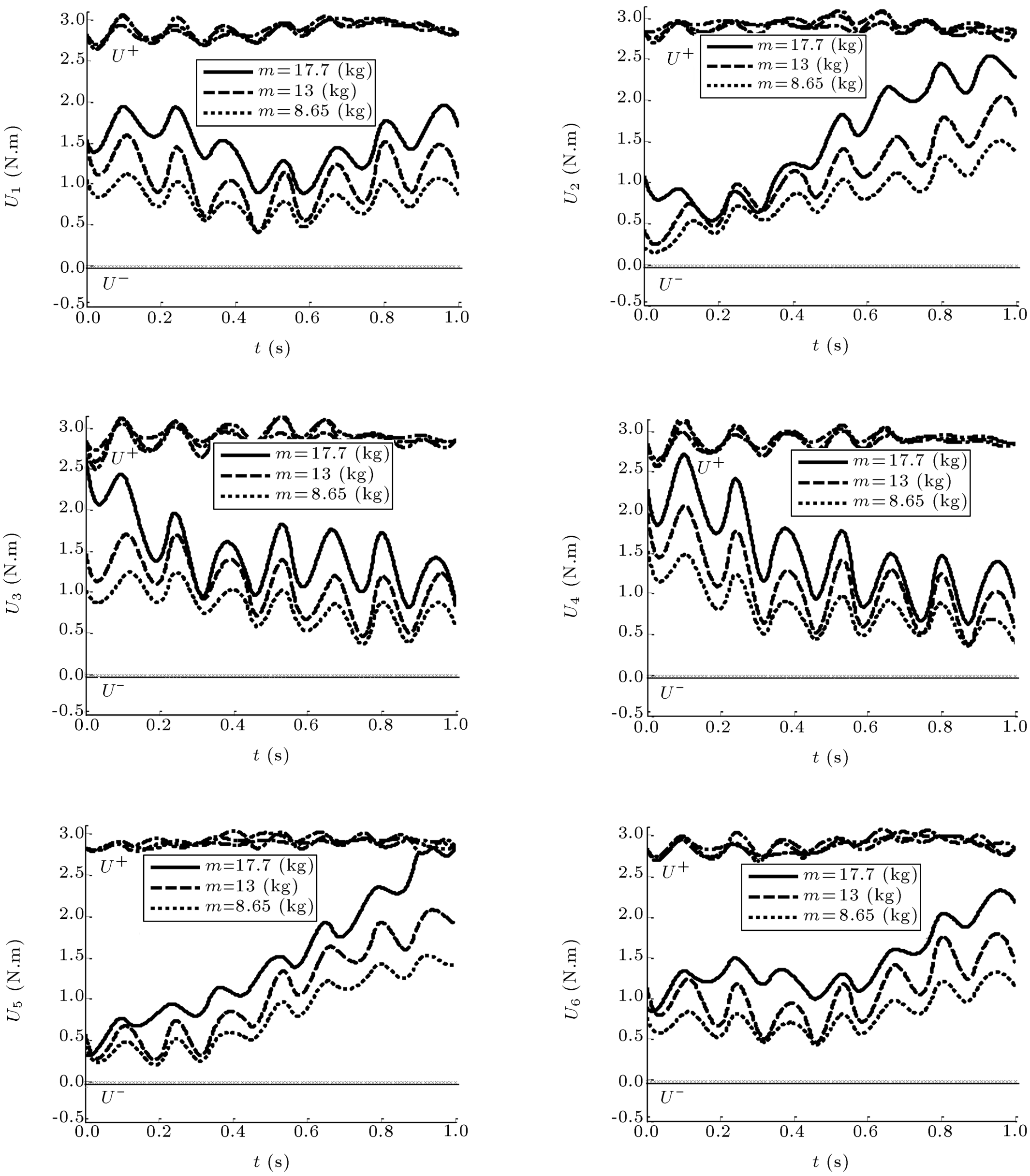

Figure 5. Diagram of motor torques to reach maximum payload for $K = 5$ (N.m/rad).

dentally, by increasing spring stiffness and, technically, decreasing the flexibility of the system, the vibrations of the motor torques are reduced and the maximum load carrying capacity is also increased.

VERIFICATION

In this paper, the proposed algorithm has been demonstrated as a promising way to predict the payload capacity. It is more uncertain and challenging for field implementation. Therefore, it is urged that field verification of the result should be carried out.

In [12], direct and indirect kinematic and dynamic modeling of one 6 cable spatial robot, considering the flexibility of joints, is undertaken. In this reference, the author has used a Matlab simulink toolbox and, then, verified the results with Sim-Designer software.

For verification of our result, first, for a specific payload, the optimal path and motor torque are found from the optimal control program. Then, the obtained optimal path is given to the inverse dynamic program [10] and the motor torque is obtained. Finally, the motor torques obtained from the two methods are compared.

It can be observed that the parameter of simulation is according to Table 2, and the boundary conditions are as in Table 1. A comparison of results for a 8.65 (kg) payload and a spring stiffness of

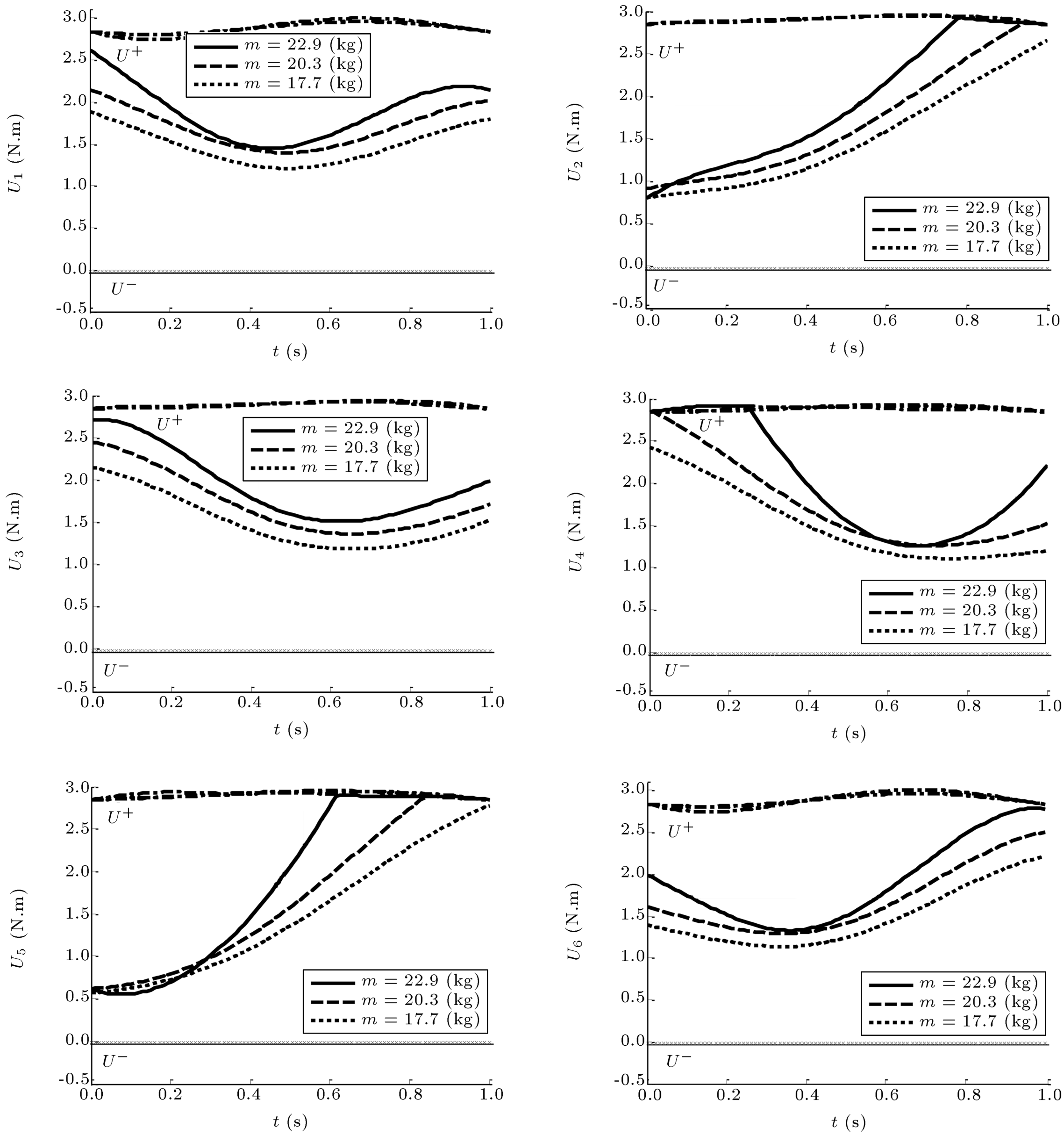

Figure 6. Diagram of motor torque reaching maximum payload in a rigid case.

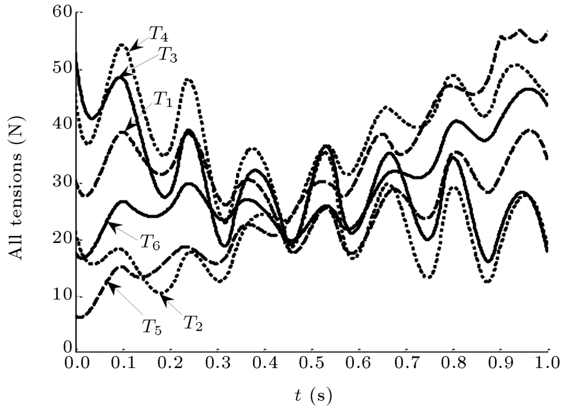

Figure 7. Cable tension in maximum payload for $K = 5$ (N.m/rad).

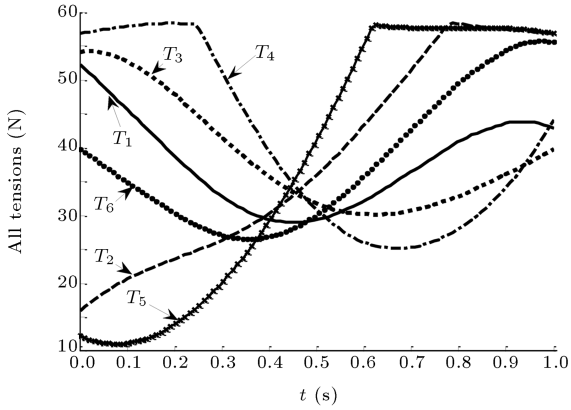

Figure 8. Cables tension in maximum payload for rigid case.

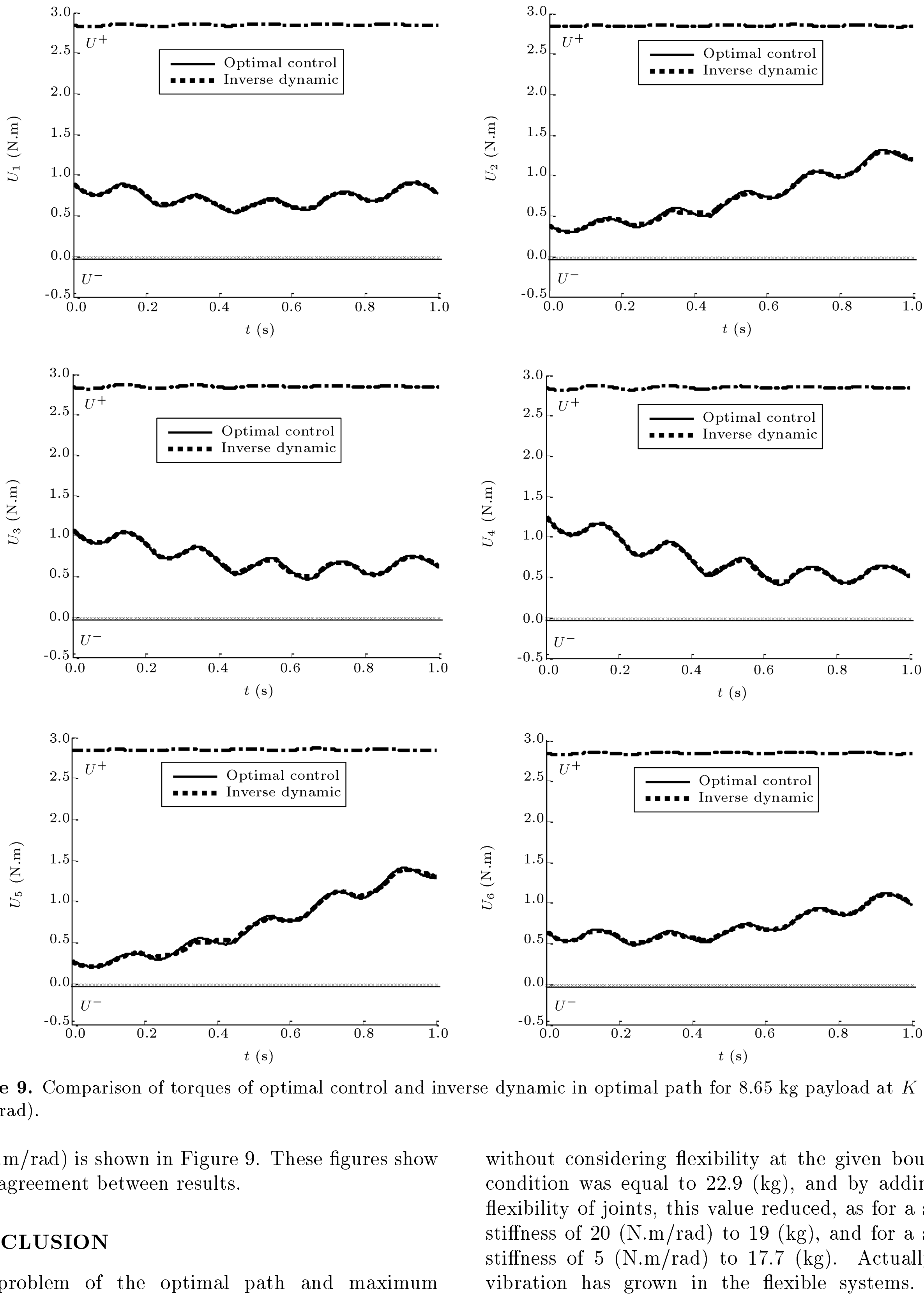

Figure 9. Comparison of torques of optimal control and inverse dynamic in optimal path for 8.65 kg payload at $K = 20$ (N.m/rad).

20 (N.m/rad) is shown in Figure 9. These figures show good agreement between results.

CONCLUSION

The problem of the optimal path and maximum carrying capacity of a 6 DOF spatial cable robot was studied. Considering flexibility of joints, the simulation was undertaken. This paper deals with the verification of results. The maximum payload without considering flexibility at the given boundary condition was equal to 22.9 (kg), and by adding the flexibility of joints, this value reduced, as for a spring stiffness of 20 (N.m/rad) to 19 (kg), and for a spring stiffness of 5 (N.m/rad) to 17.7 (kg). Actually, the vibration has grown in the flexible systems. The actuators saturation bounds are fixed for both flexible and rigid models. Meanwhile, for controlling the vibration of the end-effector, the maximum value of the produced torque in a flexible system versus a rigid case is increased. It can be shown that this indirect method is suitable for high degree of freedom systems and, moreover, can optimize some objective function simultaneously.

NOMENCLATURE

$D(X)$	inertia matrix of the manipulator
$G(X)$	vector of gravity forces
$C(X,\dot{X})$	vector of Coriolis and Centrifugal forces
$J(X)$	matrix of robot Jacobian
l	vector of cable length
a	half distance between points A & B on base of robot
b	half distance between points D & F on end-effector
K	diagonal joints stiffness matrix
j	diagonal pulleys inertia matrix
j'	diagonal motors inertia matrix
β	vector of pulley rotation angle
β'	vector of motor rotation angle
r	radius of pulleys
$\tau,$	vector of motors torque
$U(t)$	control function
τ_s	stall torque of motor
ω_m	maximum no load speed of motor
T	vector of cable tension
$J_0(U)$	objective function
H	Hamiltonian function
U_i^+, U_I^-	extrimal bound of motor torque
$\overline{U}$	vector of admissible control torque
X_1, X_2 X_3, X_4	state vectors
$W_1, W_2,$ $W_3, W_4,$ W_p, W_v, R	weighting matrices
$\psi_1, \psi_2,$ ψ_3, ψ_4	costate vectors
ε	desired accuracy in TPBVP solution

REFERENCES

1. Korayem, M.H. and Bamdad, M. "Dynamic load carrying capacity of cable-suspended parallel manipulators", *Int. J. Adv. Manuf. Technol.*, **44**, pp. 829-840 (2009).
2. Korayem, M.H. and Shokri, M. "Maximum dynamic load carrying capacity of a 6UPS-Stewart platform manipulator", *Scientia Iranica*, **15**(1), pp. (2008).
3. Wang, L.T. and Ravani, B. "Dynamic load carrying capacity of mechanical manipulators: II. Computational procedure and applications", *J. Dyn. Syst. Meas. Control*, **110**, pp. 53-61 (1988).
4. Korayem, M.H. and Nikoobin, A. "Formulation and numerical solution of robot manipulators in point-to-point motion with maximum load carrying capacity", *Scientia Iranica, Trans. B*, **16**(1), pp. 101-109 (2009).
5. Hiller, M., Fang, S., Mielczarek, S., Verhoeven, R. and Franitza, D. "Design, analysis and realization of tendon-based parallel manipulators", *J. of Mechanism and Machine Theory*, **40**(4), pp. 429-445 (2005).
6. Alp, A.B. "Cable-suspended parallel robots", MS Thesis in Mechanical Engineering at the University of Delaware (2001).
7. Korayem, M.H., Bamdad, M. and Bayat, S. "Optimal trajectory planning with dynamic load carrying capacity of cable-suspended manipulator", *IEEE International Symposium Mechatronics and Its Applications*, ISMA, pp. 1-6 (2009).
8. Korayem, M.H., Bayat, S. and Bamdad, M. "Maximum payload of cable-based planar manipulator for two given end points of end-effector using optimal control approach", *17th. Annual International Conference on Mechanical Engineering ISME*, University of Tehran (2009).
9. Korayem, M.H. and Nikoobin, A. "Maximum payload for flexible joint manipulators in point-to-point task using optimal control approach", *Int. J. Adv. Manuf. Technol.*, **38**(9/10), pp. 1045-1060 (2007).
10. Korayem, M.H., Heidari, A. and Nikoobin, A. "Effect of payload variation on the residual vibration of flexible manipulators at the end of the given path", *Scientia Iranica, Transaction B: Mechanical Engineering*, **16**(4), pp. 332-343 (2009).
11. Korayem, M.H. and Bamdad, M. "Stiffness modeling and stability analysis of cable-suspended manipulators with elastic cable for maximum load determination", *Kuwait J. Sci. Eng.*, **35**, pp. 1-21 (2010).
12. Iranpoor, M. "Modeling and simulation of kinematic and dynamic of cable actuated robot", MS Thesis in Mechanical Engineering at the Iran University of Science and Technology (2009).

BIOGRAPHIES

Moharam Habibnejad Korayem was born in Tehran, Iran, in 1961. He received his BS (Hon) and MS degrees in Mechanical Engineering from Amirkabir University of Technology, in Iran, in 1985 and 1987, respectively. He obtained his PhD degree in Mechanical Engineering from the University of Wollongong, Australia, in 1994. He is Professor of Mechanical Engineering at the Iran University of Science and Technology, where he has been involved with teaching and research activities in the area of robotics for the last 15 years.

His research interests include: Dynamics of Elastic Mechanical Manipulators, Trajectory Optimization, Symbolic Modeling, Robotic Multimedia Software, Mobile Robots, Industrial Robotics Standard, Robot Vision, Soccer Robot, and the Analysis of Mechanical Manipulators with Maximum Load Carrying Capacity. He has published more than 300 papers in international journals and conference proceedings in the field of robotics.

Ehsan Davarzani was born in Tehran, Iran, in 1984. He received his BS degree in Mechanical Engineering from Tehran University in 2007 and his MS degree from the Iran University of Science and Technology in 2009. His research interests include: Robotic Systems, Optimization, Parallel Manipulators, and Hydraulic Systems.

Mehdi Bamdad was born in Sabzevar, Iran, in 1982. He received his BS in Mechanical Engineering from KNT University of Technology, Iran, in 2004, and his MS degree from Semnan University, Iran, in 2006. He is now a PhD candidate in Mechanical Engineering at the Iran University of Science and Technology. His research interests include: Robotic Systems, Optimization, Parallel Manipulators, Industrial Automation and Mechatronic Systems.